

LETTER • OPEN ACCESS

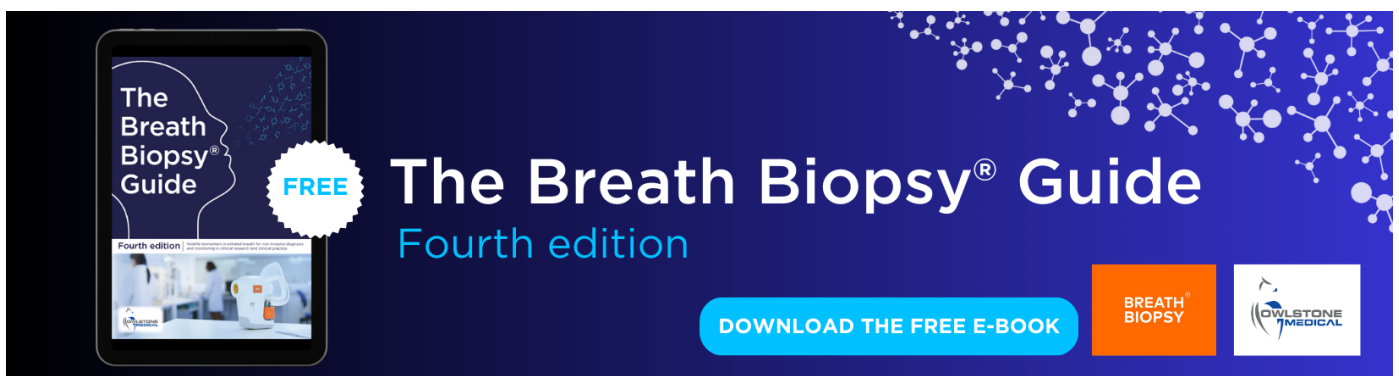
## Ignoring variation in wood density drives substantial bias in biomass estimates across spatial scales

To cite this article: Jørgen S Sæbø *et al* 2022 *Environ. Res. Lett.* **17** 054002

View the [article online](#) for updates and enhancements.

You may also like

- [\(Invited\) Manufacturable Deposition of Two-Dimensional Tungsten Disulfide for Logic Applications](#)  
Benjamin Groven, Y. Shi, P. Morin *et al.*
- [\(Invited\) Cluster-Preforming-Deposited Si-Rich W Silicide: A New Contact Material for Advanced CMOS](#)  
Naoya Okada, Noriyuki Uchida, Shinichi Ogawa *et al.*
- [Application of the Spectral Line-based Weighted-Sum-of-Gray-Gases model \(SLWSGG\) to the calculation of radiative heat transfer in steel reheating furnaces firing on low heating value gases](#)  
P D Nguyen, A Danda, M Embouazza *et al.*



The Breath Biopsy® Guide  
Fourth edition

FREE

DOWNLOAD THE FREE E-BOOK

BREATH BIOPSY

OWLSTONE MEDICAL

ENVIRONMENTAL RESEARCH  
LETTERS

## LETTER

## Ignoring variation in wood density drives substantial bias in biomass estimates across spatial scales

## OPEN ACCESS

## RECEIVED

10 May 2021

## REVISED

12 March 2022

## ACCEPTED FOR PUBLICATION

30 March 2022

## PUBLISHED

19 April 2022

Original content from this work may be used under the terms of the [Creative Commons Attribution 4.0 licence](#).

Any further distribution of this work must maintain attribution to the author(s) and the title of the work, journal citation and DOI.



Jørgen S Sæbo<sup>1,\*</sup> , Jacob B Socolar<sup>1</sup> , Edicson P Sánchez<sup>2</sup> , Paul Woodcock<sup>3</sup>, Christopher G Bousfield<sup>2</sup> , Claudia A M Uribe<sup>4</sup> , David P Edwards<sup>2</sup>  and Torbjørn Haugaasen<sup>1</sup> 

<sup>1</sup> Faculty of Environmental Sciences and Natural Resource Management, Norwegian University of Life Sciences, 1432 Ås, Norway

<sup>2</sup> Ecology and Evolutionary Biology, School of Biosciences, University of Sheffield, Sheffield S10 2TN, United Kingdom

<sup>3</sup> Joint Nature Conservation Committee, Monkstone House, Peterborough PE1 1JY, United Kingdom

<sup>4</sup> Instituto de Investigación de Recursos Biológicos Alexander von Humboldt, Villa de Leyva, Colombia

\* Author to whom any correspondence should be addressed.

E-mail: [Jorgen.sand.sabo@nmbu.no](mailto:Jorgen.sand.sabo@nmbu.no)

**Keywords:** biomass, carbon, wood specific gravity, wood density, tropical forest, Colombia, LiDAR

Supplementary material for this article is available [online](#)

**Abstract**

Rapid development of remote sensing and Light Detection and Ranging (LiDAR) technology has refined estimates of tree architecture and extrapolation of biomass across large spatial scales. Yet, current biomass maps show significant discrepancies and mismatch to independent ground data. A potential obstacle to accurate biomass estimation is the loss of information on wood density, which can vary at local and regional scales, in the extrapolation process. Here we investigate if variation in wood specific gravity (WSG) substantially impacts the distribution of above-ground biomass (AGB) across a range of scales from local plots to large regions. We collected wood cores and measured tree volume in 341 forest sites across large altitudinal and climatic gradients in Colombia. At all spatial scales, variation in WSG was substantial compared to variation in volume. Imputing study-wide average values of WSG induced regional biases in AGB estimates of almost 30%, consequently undervaluing the difference between forest areas of low and high average wood density. Further, neither stem size nor climate usefully predicted WSG when accounting for spatial dependencies among our sampling plots. These results suggest that remote sensing- and LiDAR-based projections to biomass estimates can be considerably improved by explicitly accounting for spatial variation in WSG, necessitating further research on the spatial distribution of WSG and potential environmental predictors to advance efficient and accurate large-scale mapping of biomass.

**1. Introduction**

The world's forests contain the largest pool of carbon in the biosphere (Bar-On *et al* 2018) and play an essential role in the global carbon budget (Pan *et al* 2011, Friedlingstein *et al* 2019). Carbon-focused conservation programs have been established to mitigate increasing levels of atmospheric carbon dioxide (Houghton *et al* 2015). For instance, multilateral REDD+ initiatives have raised more than 5 billion US dollars to incentivise reduction of tropical deforestation and forest degradation (Watson *et al* 2021). However, large uncertainties remain in the forest carbon stock estimates that underpin such

programs (Avitabile *et al* 2016, Réjou-Méchain *et al* 2019, Ploton *et al* 2020).

Quantification of forest biomass traditionally is based directly on inventory data, but rapid development of remote sensing and LiDAR technologies provides new opportunities for accurate and automated measurements of forest structure, from individual tree architecture (Raumonen *et al* 2013, Kellner *et al* 2019) to regional and global stand-level estimates (Saatchi *et al* 2011, Baccini *et al* 2012, Asner and Mascaro 2014, Ferraz *et al* 2016). Such remote sensing techniques can provide tree volume estimates across large spatial scales, but lack the ability to detect variation in xylem densities, commonly represented

as wood specific gravity (WSG): the oven-dry mass per unit water-saturated volume of wood, relative to the density of water (Williamson and Wiemann 2010). Species-average values range from 0.1 to 1.4 (Zanne *et al* 2009) and have an approximately multiplicative effect on individual tree biomass (Chave *et al* 2014), independent of volume (Phillips *et al* 2019). Any correlation between WSG and height or diameter of individual trees is weak or absent (Wittmann *et al* 2006, Martínez-Cabrera *et al* 2011, Fan *et al* 2012, Hietz *et al* 2017, Ubuy *et al* 2018, Phillips *et al* 2019). This absence of correlation extends to the scale of plots, where total basal area and LiDAR derived top-of-canopy height carry insufficient information to predict average WSG (Asner *et al* 2012, Jucker *et al* 2018a, Muñoz Mazón *et al* 2020).

Two pantropical maps of forest biomass derived from satellite LiDAR data and wall-to-wall remote sensing products (Saatchi *et al* 2011, Baccini *et al* 2012) have been widely applied as reference data in ecological studies (Sullivan *et al* 2020, Walker *et al* 2020, Wigneron *et al* 2020). However, the maps contain spatial discrepancies with one another (Mitchard *et al* 2013) and interregional biases when compared to independent ground plots (Mitchard *et al* 2014, Avitabile *et al* 2016). Information on spatial variation in WSG could be lost in the intermediate LiDAR step between sparse plot data and continuous remotely sensed data as neither pantropical analysis accounts for any intracontinental differences in the relationship between above-ground biomass (AGB) and LiDAR-detected forest structure (Saatchi *et al* 2011, Baccini *et al* 2012). However, such a role of WSG in promoting the observed inconsistencies is debated (Mitchard *et al* 2014, Saatchi *et al* 2014).

Ground-plot studies have demonstrated differences in community-weighted WSG between distant tropical regions (ter Steege *et al* 2006, Asner and Mascaro 2014), and local differences up to 20% between adjacent forests induced by shifting substrate properties (Baraloto *et al* 2011, Gourlet-Fleury *et al* 2011, Phillips *et al* 2019) and flooding regimes (Hawes *et al* 2012, de Assis *et al* 2019, Mori *et al* 2019). But the degree to which such spatial variation in WSG control biomass, and how it emerges and develops across intermediate spatial scales, is unclear. Previous assessments of biomass estimation error driven by omission of spatial variation in WSG show contrasting results (Asner *et al* 2012, Mitchard *et al* 2014, Saatchi *et al* 2014, Phillips *et al* 2019), but the studies diverge on the spatial scaling of analyses and weighting of upscaled WSG, and fail to account for potential spatially contingent bias introduced by intra-specific variation (Patiño *et al* 2009, Bredin *et al* 2020).

The spatial scale at which extrapolated biomass estimates are most reliable thus depends on the magnitude and scale at which average WSG varies and our ability to capture and retain such variation through extrapolation processes. In this study, we investigate

the spatial pattern of variation in WSG across Colombia, quantify the relative errors induced on AGB estimates at different spatial scales when neglecting spatial variation in WSG, and explore the potential of environmental correlates to predict WSG across space. We address the current knowledge gap by explicitly assessing variance manifesting at different spatial scales and assuring relevance for biomass estimation and integration of intra-specific effects by applying volume-weighting of average WSG values and relying on locally collected WSG measurements.

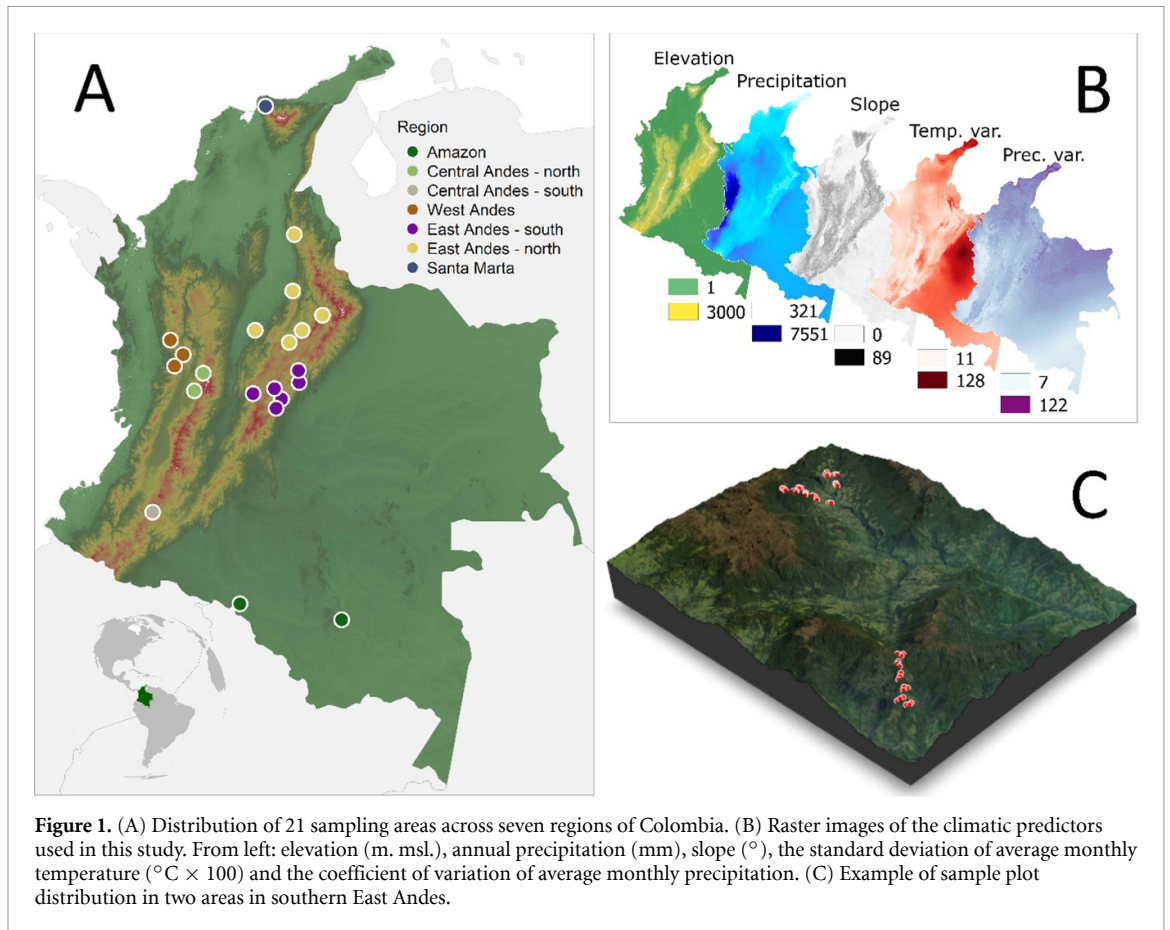
## 2. Methods

### 2.1. Spatial arrangement of study sites

We established 341 forest plots (75 m<sup>2</sup> in West Andes, 300 m<sup>2</sup> in all other regions) across seven broad biogeographic regions of Colombia: The lowland Amazon ( $n = 46$ , elevation = 133–288 m. msl.), the northern West Andes ( $n = 83$ , elevation = 1142–2684 m. msl.), the northern Central Andes ( $n = 12$ , elevation = 1754–2699 m. msl.), the southern Central Andes ( $n = 9$ , elevation = 2691–3360 m. msl.), the northern East Andes ( $n = 72$ , elevation = 119–3381 m. msl.), the southern East Andes ( $n = 113$ , elevation = 1163–3415 m. msl.) and the Sierra Nevada de Santa Marta ( $n = 6$ , elevation = 1891–2606 m. msl.). Within these regions, the plots were further grouped on two intermediate spatial scales. First, all plots were grouped in clusters of three. Individual plots were separated by 70–230 m, while clusters were separated by at least 370 m (figure 1(C)). Second, all plots closer than 20.5 km to each other were grouped into 21 different areas, with all areas separated by at least 22.5 km and each comprising 6–44 plots (figure 1(A)). This hierarchical grouping aggregated our forest structure data on four spatial scales, from plots (<30 m), through clusters (<600 m), areas (<20.5 km) and biogeographic regions.

The large-scale distribution of plots was selected haphazardly based on research permits and the access to primary and mature secondary forest at each location. Local scale plot placement was chosen without reference to the plot-scale forest structure or terrain except where the terrain constrained options for access on foot. Plot coordinates were determined by handheld GPS. For each plot, we extracted climatic variables from the WorldClim ver. 2 database (Fick and Hijmans 2017) and elevation and topographic slope from the AW3D30 ver. 2.2 dataset (Tadono *et al* 2014).

The sample plots spanned an elevational gradient from 133 to 3415 m above sea level. The total annual precipitation ranged from 910 to 3128 mm and the coefficient of variation of monthly precipitation ranged from 19.2% to 73.9%. Mean annual temperature ranged from 8.2 °C to 27.2 °C and showed strong correlation with elevation (Pearson's  $r = -0.99$ ), and the standard deviation of average



monthly temperatures ranged from  $0.2^{\circ}\text{C}$  to  $0.76^{\circ}\text{C}$ . Within areas, plots spanned an elevational range of 507 m on average (range 38–1243 m), and an average annual precipitation range of annual precipitation of 298 mm (range 18–933 mm; supplementary methods, table S1-1 available online at [stacks.iop.org/ERL/17/054002/mmedia](https://stacks.iop.org/ERL/17/054002/mmedia)).

## 2.2. Field measurements

Within each plot, we measured the diameter at breast height (DBH) for all trees greater than 5 cm DBH. We estimated individual tree volume using the tree volume term from the Alvarez *et al* (2012) type II.4 biomass equation, which was developed from a dataset on felled trees across a range of forest types in Colombia.

Wood cores were extracted (two threads, 5.15 mm; Haglöf, Sweden) for a subset (mean = 44%) of trees in each plot. We collected taxonomic information for a limited number of stems ( $n = 28.4\%$ ) belonging to locally dominant species (*Quercus humboldtii*,  $n = 776$ ; plot-specific morphospecies,  $n = 192$ ; cluster-specific morphospecies,  $n = 19$ ), and cored only a subset of each (*Quercus humboldtii*,  $n = 43$ ; morphospecies,  $n = 2$ –5 per plot or cluster) (see supplementary methods, figure S1-1). We attempted to extract cores from all the largest trees in each plot and the largest individuals of each morphospecies, while the remainder of stems were cored at

random (see supplementary methods, figure S1-2). The wood density ( $\rho_{\text{wood}}$ ) of the core was measured as the dry weight to wet volume ratio ( $\text{g cm}^{-3}$ ), after removing the bark and pith from the sample. WSG is given as the unitless, standardized density of wood relative to the density of water ( $\rho_{\text{water}} = 1 \text{ g cm}^{-3}$ ). Cores were rehydrated prior to volume measurement and dried at  $105^{\circ}\text{C}$  for at least 60 h before weighting (Díaz *et al* 2016). All field data is available online at <https://data.mendeley.com/datasets/zzzzcnt2bd/1> (Sæbø 2022).

## 2.3. Statistical analysis

### 2.3.1. Stem-level variation in WSG

We fit a linear mixed-effects regression model on the stem-level WSG data to investigate stem-level variation in WSG across our study, test for any size-WSG relationships that could support the use of LiDAR for biomass extrapolation, and derive uncertainty-bounded estimates of WSG for uncored trees for further analysis. The full model for each WSG measurement  $i$  is

$$\text{WSG}_i = \alpha + \beta_{\text{plot}[j]} + \beta_s \times \text{species}_i \times \text{ID}_i + \beta_v \times \text{volume}_i + \varepsilon_{i(\text{ID}=1)} \times \text{ID}_i + \varepsilon_{i(\text{ID}=0)} \times (1 - \text{ID}_i)$$

$$\beta_{\text{plot}[j]} \sim N(\beta_{\text{cluster}[j]}, \tau_{\text{cluster}})$$

$$\beta_{\text{cluster}} \sim N(\beta_{\text{area}[k]}, \tau_{\text{area}})$$

where  $\alpha$  is the overall intercept,  $\beta_v$  is a fixed effect of the tree's volume,  $\beta_{\text{plot}[i]}$  is a plot-specific random effect centred on a cluster-specific random intercept  $\beta_{\text{cluster}[j]}$ , and where cluster  $j$  is centred on an area-specific random effect  $\beta_{\text{area}[k]}$  for area  $k$ . To avoid potential sampling bias due to plots with dominant tree species, the limited taxonomic information was added as an additional random effect  $\beta_s$  for identified trees. The Boolean variable *ID* excludes this random effect for unidentified trees. As the intra-specific variances are captured in the  $\beta_s$  random effect for identified trees only, we allowed separate variances for identified and unidentified trees.

### 2.3.2. Contribution of WSG to variation in above-ground biomass

We multiplied each plot's total tree volume by the plot-level volume-weighted WSG estimate (calculated as the uncertainty-bound volume-weighted average WSG of all stems in the plot) to derive final plot-level values of AGB in  $\text{t ha}^{-1}$ . We then used two strategies to assess how strongly variation in WSG contributes to the variation in AGB at different spatial scales. First, we calculated the between-plot coefficient of variation of AGB, WSG and volume within each region and across the study extent to assess their relative contribution to the variation in estimated AGB. We further calculated the between-cluster and between-area coefficients of variation across the study extent to indicate the relative change in variation in WSG and volume among sample units of different spatial extents.

Second, we calculated the deviation between the volume-weighted WSG of individual spatial units and the volume-weighted average of the spatially superior unit (leaving out the unit of interest). For example, the observed deviation for the Amazon region was calculated as its volume-weighted WSG subtracted from the volume-weighted WSG of all other regions, while for an area within the Amazon it was calculated as its volume-weighted WSG subtracted from the volume-weighted WSG of all other areas within the Amazon. Proportional deviation was represented as the deviation relative to the observed WSG, and absolute deviations as the magnitude of the resulting differences in AGB estimates.

We judged whether these observed deviations significantly exceeded expectations from sampling variation alone by the 95% intervals of the differences between the observed WSG at each unit and a null distribution generated under the assumption of no spatial effects occurring at the spatial scale in question. We generated these null distributions for the volume-weighted WSG value of each spatial unit by repeatedly ( $n = 4000$ ) resampling (with replacement)

the volume-weighted WSG values of spatially subordinate units from the pool within the spatially superior unit (excluding the unit being tested), with each new sample consisting of the same number of subordinate units as the original unit being tested. For example, the null distribution for the Amazon region was generated by repeatedly drawing two areas (the number of areas in the Amazon) from all other regions with replacement, while the null distribution for an area within the Amazon was generated by repeatedly drawing eight clusters from all other areas in the Amazon with replacement.

We repeated the above procedure for clusters, areas and regions. Spatial units were ranked from subordinate to superior according to their spatial scale (i.e. from plots to clusters, areas, regions and the overall study area).

### 2.3.3. Predicting WSG from environmental variables

We regressed plot-level volume-weighted WSG on elevation, total annual precipitation, the coefficient of variation of average monthly precipitation, the standard deviation of monthly average temperature, and the topographic slope.

The Moran's I statistic indicated strong spatial autocorrelation in the model residuals. Therefore, we cross-validated the model while accounting for the spatial structure of the data.  $K$ -fold cross-validation divides the data into a number ( $k$ ) of 'folds'. The model is refit  $k$  times on  $k-1$  folds, iteratively calculating predictions and model performance statistics for the excluded fold. In leave-one-out cross validation, we iteratively excluded one of the 341 individual plots, while in larger fold cross-validation, we divided the data into folds corresponding to the size of clusters (108-fold), areas (23-fold) and regions (7-fold). To track the effect of spatial dependence on validation estimates, we performed a 'random' cross-validation for each fold size that assumed spatial independence among residuals, and a 'spatial' cross-validation that retained the spatial structure of the data.

Additionally, we fit a second model that included the same environmental covariates as well as random effects of either cluster or area. We compared these models to a model that included random effects while omitting the environmental predictors.

### 2.3.4. Model fitting and error propagation

We fit the models in JAGS (Plummer 2003) via R package jagsUI (Kellner 2019). We used weakly informative gamma priors (shape = 1, rate = 0.001) on all precision hyperparameters and normal priors (mean = 0–0.5, precision = 1–2) on all random effect parameters (see supplementary methods S1 and table S1-2 for the reasoning justification of our priors). We ran all models on four chains for a function-optimized number of adaptation iterations (Kellner

2019). The individual tree model ran for 10 000 burn-in iterations and 50 000 sampling iterations, saving every 50th iteration for a total of 4000 posterior samples. Plot-level models ran for 1000 warm-up and 10 000 (models without spatial effects) or 50 000 (models with spatial effects) sampling iterations. Every 10th or 50th sample were saved for a total of 4000 combined posterior samples across the iteratively fit models. Model fit and convergence was assessed using graphical predictive checks and the Gelman–Rubin  $R$ -hat estimator (Gelman and Rubin 1991).

Model performance was assessed from posterior estimates of the root mean squared error (RMSE), the squared Pearson correlation between model fitted and observed WSG ( $R^2$ ) and deviance information criterion (DIC). Predictive performance of cross-validated models was assessed from posterior estimates of the expected log predictive density (elpd), the root of average squared prediction errors (RMSPE), and the squared Pearson correlation between model predicted and observed WSG ( $pR^2$ ).

Uncertainty in stem-level WSG values was propagated through consecutive analysis by repeating all procedures across an array of volume-weighted plot-average WSG combining the field measurements for cored trees with 100 posterior draws from the final stem-level model for non-cored trees.

### 3. Results

#### 3.1. Spatial variation in stem-level WSG

The distribution of WSG, DBH, and tree volume estimates showed variation across our study sites (figure 2, supplementary methods, table S1-1). The relationship between individual tree volume and WSG was not detectably different from zero (figure 1(D), supplementary results, table S2-1). RMSE and Bayesian  $R^2$  estimates indicated large residual variation and weak predictive capabilities at the individual tree level (supplementary results, table S2-1 and figure S2-1). However, the correlation between estimated and raw plot-level volume-weighted WSG was strong (Pearson's  $r = 0.95$ ), indicating that our results do not hinge heavily on imputed WSG values for uncored stems (supplementary results, figure S2-1). The model estimated that around 60% of the spatial variance in stem-level WSG occurred between the 21 areas, 14% occurred between clusters within areas, and 26% occurred between plots within clusters (figure 3, supplementary results, table S2-1). The estimated random intercepts of spatial units of different regions overlapped but showed clear overall differences, with the Amazon portraying consistently high and the central Andean regions consistently low WSG at all spatial levels (figure 3).

#### 3.2. Effect on above-ground biomass estimates of ignoring variation in WSG

The regional-scale AGB ranged from 307.4 t ha<sup>-1</sup> in the lowland Amazon to 117.3 t ha<sup>-1</sup> in the highest-altitude areas in the southern Central Andes (~3000 m. msl., table 1). The coefficient of variation was mainly driven by large variations in tree volume, but the additional variability due to WSG was substantial. The between-area coefficient of variation was 32% of that of tree volume across the study extent (table 1). The variation in volume increased more substantially than the variation in WSG at smaller scales (table 1), indicating that the control of WSG on spatial patterns of biomass increase with increasing scales. Average volume weighted WSG ranged from 0.40 to 0.58 at the scale of regions, resulting in substantial deviations between individual regions and the full dataset (figure 4). Replacing region-specific WSG values with the overall average WSG value led to relative errors of up to 29% and absolute AGB errors of up to 41.4 t ha<sup>-1</sup> (supplementary results, table S2-3, Central Andes north and Amazon, respectively). Area-level volume weighted WSG ranged from 0.37 to 0.63 s across the dataset and showed inter-regional spans of up to 0.09, resulting in inter-regional errors of up to 17% and 50.4 t ha<sup>-1</sup> (supplementary results, table S2-4, Amazon area II and I). Cluster-level volume-weighted WSG ranged from 0.34 to 0.74 across the dataset and showed inter-area spans of up to 0.22, resulting in inter-area errors of up to 30% and 69.6 t ha<sup>-1</sup> (supplementary results, table S2-5, East Andes north VI cluster XI and West Andes I cluster I).

The null model approach demonstrated the existence of spatially driven variation among regions, beyond patterns of random variation and subscale covariance. The average WSG of three regions fell outside the expected value under the scenario of no spatial effect above the area level (figure 4, supplementary results, table S2-3). Spatial patterns at smaller scales were generally more consistent with null variation, but some spatial effects at the level of areas and clusters were indicated within the Amazon, northern Central Andes and West Andes. A total of five areas (supplementary results, table S2-4) and nine clusters (supplementary results, table S2-5) deviated significantly from their null distributions.

#### 3.3. Predicting plot average WSG from environmental variables

The non-spatial and cluster random effect models for plot-level volume-weighted WSG estimated significant decreases in volume-weighted WSG along the elevational gradient of 0.035 and 0.039 per 1000 m altitude, respectively. No effects remained significant (i.e. 95% credible intervals do not overlap zero) when including random intercepts for each area

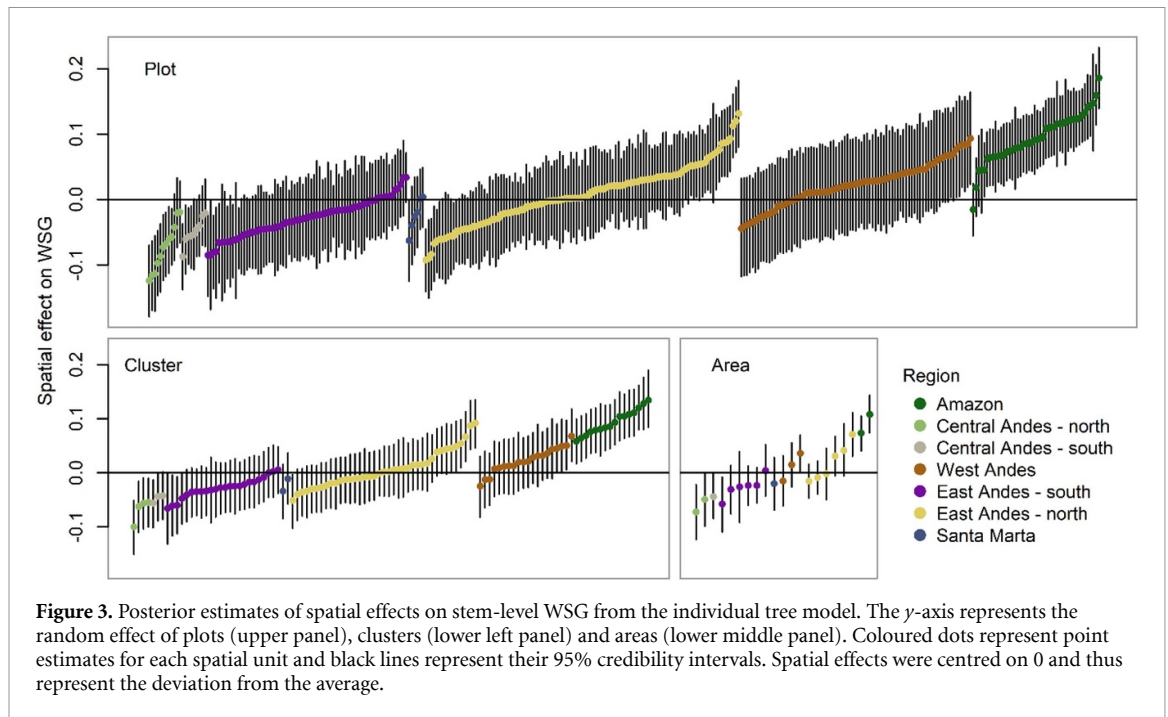
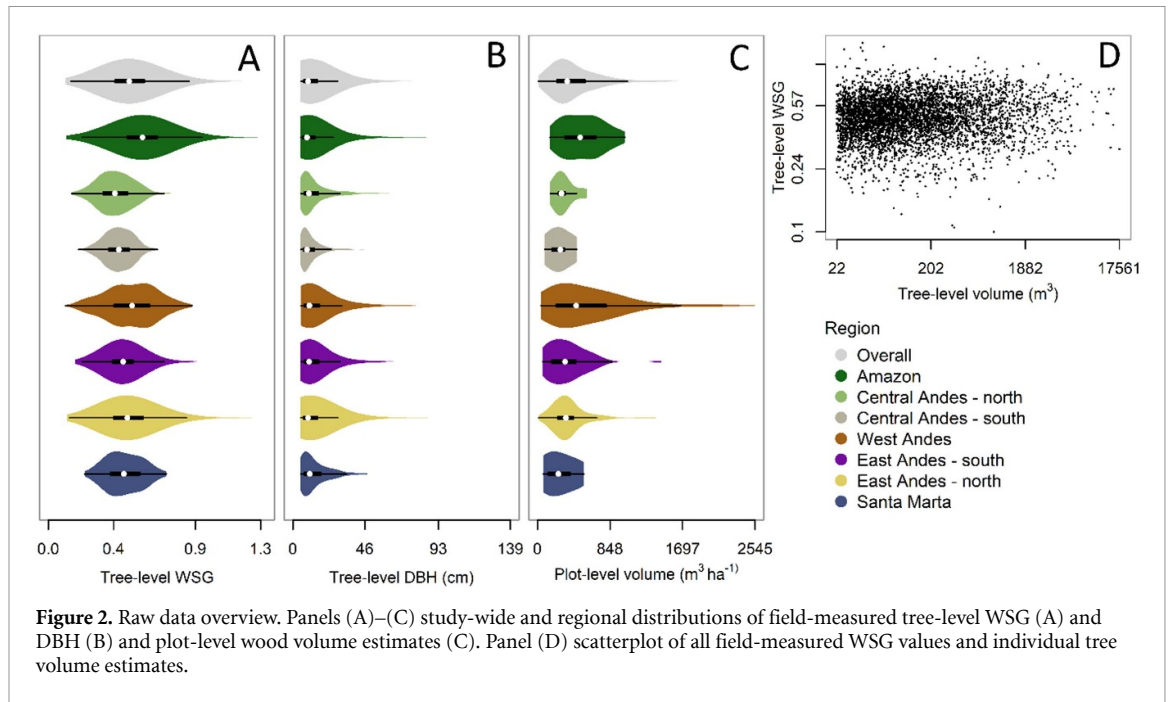


**Table 1.** AGB estimates and coefficient of variation for AGB, WSG and volume for each region.

Region	Above-ground biomass			Coefficient of variation						
	Mean	95% CI		AGB	95% CI	Volume	WSG	95% CI		
Amazon	307.4	304.4	310.3	0.47	0.47	0.48	0.45	0.15	0.14	0.16
Central Andes—north	124.1	121.8	126.4	0.49	0.47	0.5	0.4	0.13	0.1	0.16
Central Andes—south	117.3	113.8	120.8	0.51	0.48	0.54	0.52	0.08	0.06	0.1
West Andes	302.1	297.7	306.5	0.86	0.85	0.88	0.8	0.18	0.17	0.19
East Andes—south	160.2	155.7	164.8	0.69	0.64	0.75	0.66	0.13	0.11	0.15
East Andes—north	193.6	187.5	199.9	0.61	0.53	0.69	0.57	0.13	0.12	0.15
Santa Marta	129.2	126.1	132.2	0.72	0.7	0.74	0.68	0.08	0.05	0.1
Overall (between-plot)	222.7	219.9	225.4	0.79	0.78	0.81	0.73	0.17	0.16	0.17
Overall (between-cluster)				0.53	0.5	0.55	0.48	0.14	0.13	0.15
Overall (between-area)				0.43	0.42	0.44	0.37	0.12	0.11	0.13

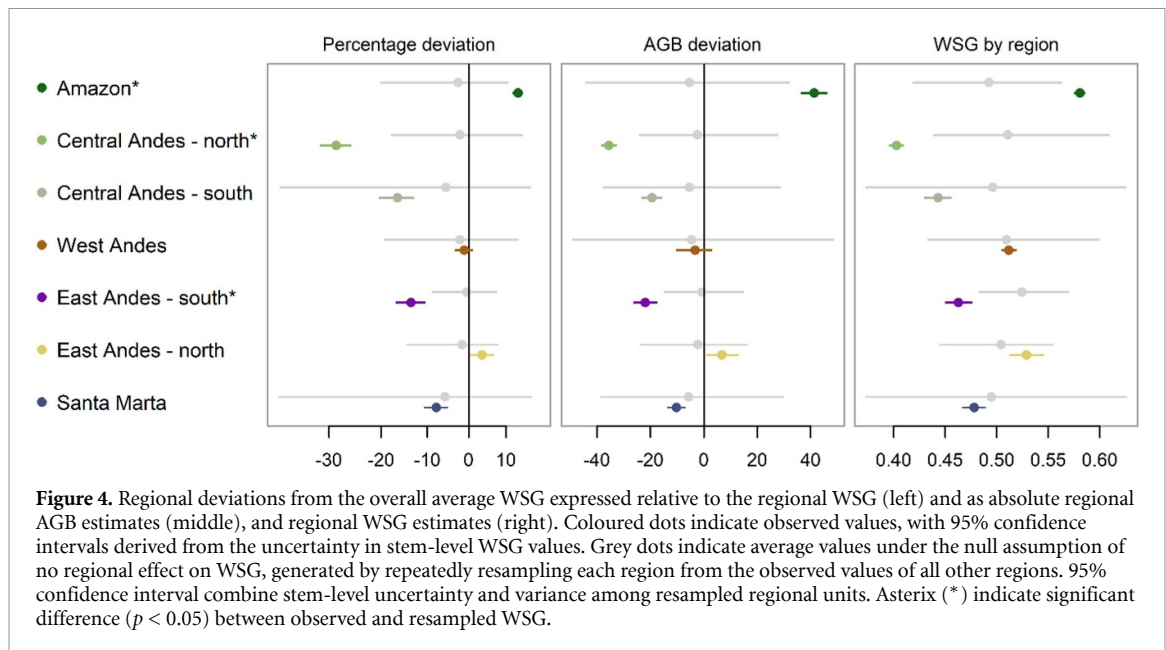


**Table 2.** Estimated expected log predictive density (elpd), root mean squared predictive error (RMSPE) and predictive  $R$ -squared ( $pR^2$ ) of the non-spatial environmental model, and elpd of the non-spatial model without environmental covariates. All model criteria are estimated from cross-validation procedures assuming spatial independence (random CV) or spatial dependence (spatial CV) among plots at different spatial levels.

$k$ -fold CV	Random CV				Spatial CV			
	elpd	Environmental model			elpd	Environmental model		
		elpd	RMSPE	$pR^2$		elpd	RMSPE	$pR^2$
Leave-one-out					356.7	374.1	0.080	0.095
108-fold (cluster)	356.6	373.9	0.080	0.095	355.6	370.3	0.081	0.082
23-fold (area)	356.5	373.9	0.080	0.096	347.6	341.0	0.087	0.026
7-fold (region)	356.8	372.6	0.081	0.090	336.1	291.5	0.096	0.018

(supplementary results, table S2-2). DIC,  $R^2$  and RMSE estimates indicated that the environmental predictors improved model fit when assuming spatial independence among the WSG estimates, but did not result in better fits than spatial models with no environmental predictors (supplementary results, table S2-2).

Cross-validation of the non-spatial model indicated that environmental covariates added little predictive power beyond through autocorrelative effects. RMSPE and  $pR^2$  estimates decreased only slightly with increasing sizes of random folds, but deteriorated strongly when cross-validating to folds accounting for spatial dependencies in the data (table 2). The model with no environmental predictors provided better predictive performance than the environmental model in terms of elpd when cross-validating across areas and regions (table 2).

## 4. Discussion

WSG differ largely among species and individuals and alters the capacity of trees to accumulate biomass, but how this variation scales up to extents relevant to forest management and interpretation of carbon

maps is poorly known. We observed that small-scale variance in stem-level WSG across diverse forests in Colombia accumulates across increasing spatial scales and substantially influences spatial variation in AGB. Consequently, ignoring the variation in WSG in our dataset across different spatial scales generated considerable regional biases in estimated AGB and an undervaluation of differences between spatial units. Comparison to null distributions assuming the absence of spatial patterning established that inter-regional differences were involved in generating the overall patterns of variance in WSG.

### 4.1. The importance of WSG in above-ground biomass estimation

LiDAR and remote sensing technologies provide us the ability to collect immense amounts of data on tree size, facilitating large-scale extrapolations of AGB estimates. However, weak and divergent relationships between WSG and tree size measurements among species database values (Martínez-Cabrera *et al* 2011, Fan *et al* 2012, Hietz *et al* 2017), field data on individual trees (Wittmann *et al* 2006, Ubuy *et al* 2018, Phillips *et al* 2019) and in aggregated plot values (Asner *et al* 2012, Jucker *et al* 2018a, Phillips *et al* 2019,

Muñoz Mazón *et al* 2020) indicate that the divergence between the pioneer strategy of rapid volumetric growth and the old-growth strategy of slower growth but higher survival rates (De Souza *et al* 2016, Hietz *et al* 2017) do not translate into any general relationship between WSG and adult tree stature. The absence of any relationship between WSG and volume in our stem-level WSG model are consistent with these previous observations, collectively establishing that spatial information on WSG is effectively ignored at scales where AGB is extrapolated across volumetric data (e.g. LiDAR data), and any predictive power contingent on this information is lost.

The implications of this conclusion depend on the degree to which WSG controls spatial patterns of AGB, but previous literature has left this question unresolved. Evaluations of the importance of WSG in spatial AGB estimation have been limited to either the scale of individual forest plots or large regions (ter Steege *et al* 2006, Asner and Mascaro 2014, Mitchard *et al* 2014, Phillips *et al* 2019), leaving it unclear how variance in WSG arise and develops across different spatial scales. Robust conclusions on the scales we evaluated here have also been impeded by confounding between estimated spatial patterns and sampling variation. This issue is evident in the contradictory results on intra-Amazon regional variation (Mitchard *et al* 2014, Saatchi *et al* 2014), demonstrating that a scarcity of field data leaves average values of WSG sensitive to collection biases, and questioning the certainty of observed differences between large-scale tropical regions (ter Steege *et al* 2006, Asner and Mascaro 2014, Phillips *et al* 2019). Further, while phylogenetic conservatism (Chave *et al* 2006) has justified the use of taxonomically coarse database values of WSG in all the above studies, considerable spatial variation have been shown to occur within species (Patiño *et al* 2009, Bredin *et al* 2020).

By partitioning the variance to a range of spatial scales across a large and varied study area, propagating uncertainty in locally collected WSG estimates through the full analysis, and explicitly disentangling spatial effects from confounding sampling variation, our results provide robust clarifications on the effect of WSG on spatial AGB distribution. Notably, the importance of WSG as a control of AGB increased at larger scales, as indicated by the increasing variance in WSG relative to that of tree volume and a clear rejection of the null hypothesis of no difference between regions. The relatively small sample sizes within individual units at smaller spatial scales left the null analysis approach with weak power to confirm spatial effects between areas and clusters, but both the stem-level and plot-level mixed models suggest that variation in WSG manifest on all spatial scales and has substantial effects on AGB distribution.

The magnitude of the observed spatial deviations in WSG and the resampled null distribution for each

spatial unit depends strongly on the overall distribution of WSG. For example, increasing the number of samples from the significantly deviating north Andes region would strengthen their dominance over the overall sample distribution, altering the regional deviations and eventually pulling all null distributions outside their regional averages. The specific distribution of bias in our results are thus of lesser interest, as our overall sample distribution does not have any concrete analogue in any biomass map. How such bias distributes in individual products depends on the distribution of the extrapolated ground data. However, the prevalence of spatial variation in WSG and resulting observed deviations demonstrate that the efficiency gains for AGB estimation presented by developing technologies such as LiDAR are constrained by our ability to capture and retain such variation through the extrapolation process, and suggests that WSG should be a target for further improvements to our mapping capabilities.

#### 4.2. Predicting WSG from environmental covariates

Detaching the extrapolation of WSG from the LiDAR framework may enable more accurate spatial estimates if appropriate correlates of WSG are identified. Stand-average WSG have previously been linked to latitude (Wiemann and Williamson 2002, Lewis *et al* 2013), elevation (Chave *et al* 2006, Slik *et al* 2010, Muñoz Mazón *et al* 2020), gradients of rainfall and temperature (Slik *et al* 2010, Lewis *et al* 2013), spatial patterns of disturbance (Slik *et al* 2010, Magnabosco Marra *et al* 2018), and distinctive soil characteristics (Baraloto *et al* 2011, Gourlet-Fleury *et al* 2011, Phillips *et al* 2019) and flooding regimes (Hawes *et al* 2012, Lewis *et al* 2013). However, such results are often weak and inconsistent across regions and scales. For example, WSG can be positively, negatively or uncorrelated with elevation in different areas, commonly interpreted as products of local differential disturbance patterns or elevational distribution of hard-wooded species (Swenson and Enquist 2007, Slik *et al* 2010, Muñoz Mazón *et al* 2020). Likewise, disturbance is generally thought to generate patterns of lowered community average WSG through promoting the establishment of early-successional species (Magnabosco Marra *et al* 2018, Aleixo *et al* 2019), but the opposite pattern has arisen following selective mortality of trees with low WSG (van Nieuwstadt and Sheil 2005, Slik *et al* 2010) more prone to implosion of conduits when facing negative water pressure (Hacke *et al* 2001) and mechanical failure inflicted by external forces (Van Gelder *et al* 2006, Niklas and Spatz 2010).

The presence of universal large-scale predictors of WSG is thus unclear. In this study, none of the climatic predictors we assessed showed appreciable ability to predictive ability, with any modest explanatory power achieved via spatial autocorrelation (Dormann

2007) rather than any relationship between WSG and the predictors (see also Ploton *et al* 2020). Substantial effort is required to attain an applicable approach to discerning spatial patterns, by disentangling the seemingly complex and context dependent relationships between WSG and potential environmental predictors, to gain a comprehensive overview of representative forest type values, or establishing direct relationships with remotely sensed reflectance imagery (Jucker *et al* 2018b).

## 5. Conclusion

We suggest that WSG requires considerable research effort in the pursuit of accurate estimates of global distributions of forest biomass. The spatial patterns of AGB within the bounds of our study were considerably regulated by WSG across all scales, demonstrating that the predictive performance and accuracy of biomass maps can be enhanced by explicitly accounting for the spatial distribution of WSG. Large-scale systematic ground sampling of WSG is needed to reveal spatial patterns on scales relevant to forest conservation and support further investigations on potential spatial predictors.

## Data availability statement

The data that support the findings of this study are openly available at the following URL/DOI: <http://dx.doi.org/10.17632/zzzcnt2bd.1>.

## Acknowledgments

We thank the biological collection department at Instituto de Investigación de Recursos Biológicos Alexander von Humboldt for providing necessary logistical support and laboratory facilities, and D Martínez, L A H Gallego, M J H Gallego, J M R Gutiérrez, L Rodríguez, A Andoke, S Terakami and local guides for invaluable collaboration in the field and lab. We also thank numerous national and private reserves, landowners and the Indigenous Andoke community of Caño Aduche for access permissions and generously sharing local knowledge. Funding was provided to D P E from the Natural Environment Research Council (Grant No. NE/R017441/1) and to T H and D P E by the Research Council of Norway (Grant No. 262378). This is article no. 24 of the Biodiversity, Agriculture and Conservation in Colombia/Biodiversidad, Agricultura, y Conservación en Colombia (BACC) project.

## Conflict of interest

The authors have no conflict of interest to declare.

## Author contribution

D P E, T H, J B S and J S S conceived the study and developed the methodology. J S S, E P S, P W and C G B collected the data with logistical support from C A M U and J B S. J S S analysed the data with input from J B S. J S S wrote the manuscript with input from all authors.

## ORCID iDs

Jørgen S Sæbo  <https://orcid.org/0000-0001-7658-4290>

Jacob B Socolar  <https://orcid.org/0000-0002-9126-9093>

Edicson P Sánchez  <https://orcid.org/0000-0003-2670-3882>

Christopher G Bousfield  <https://orcid.org/0000-0003-3576-9779>

Claudia A M Uribe  <https://orcid.org/0000-0002-7714-9220>

David P Edwards  <https://orcid.org/0000-0001-8562-3853>

Torbjørn Haugaasen  <https://orcid.org/0000-0003-0901-5324>

## References

- Aleixo I, Norris D, Hemerik L, Barbosa A, Prata E, Costa F and Poorter L 2019 Amazonian rainforest tree mortality driven by climate and functional traits *Nat. Clim. Change* **9** 384–8
- Alvarez E, Duque A, Saldarriaga J, Cabrera K, de Las Salas G, Del Valle I, Lema A, Moreno F, Orrego S and Rodríguez L 2012 Tree above-ground biomass allometries for carbon stocks estimation in the natural forests of Colombia *For. Ecol. Manage.* **267** 297–308
- Asner G P and Mascaro J 2014 Mapping tropical forest carbon: calibrating plot estimates to a simple LiDAR metric *Remote Sens. Environ.* **140** 614–24
- Asner G P, Mascaro J, Muller-Landau H C, Vieilledent G, Vaudry R, Rasamoelina M, Hall J S and van Breugel M 2012 A universal airborne LiDAR approach for tropical forest carbon mapping *Oecologia* **168** 1147–60
- Avitabile V *et al* 2016 An integrated pan-tropical biomass map using multiple reference datasets *Glob. Change Biol.* **22** 1406–20
- Baccini A *et al* 2012 Estimated carbon dioxide emissions from tropical deforestation improved by carbon-density maps *Nat. Clim. Change* **2** 182–5
- Bar-On Y M, Phillips R and Milo R 2018 The biomass distribution on Earth *Proc. Natl Acad. Sci. USA* **115** 6506–11
- Baraloto C *et al* 2011 Disentangling stand and environmental correlates of aboveground biomass in Amazonian forests *Glob. Change Biol.* **17** 2677–88
- Bredin Y K, Peres C A and Haugaasen T 2020 Forest type affects the capacity of Amazonian tree species to store carbon as woody biomass *For. Ecol. Manage.* **473** 118297
- Chave J *et al* 2014 Improved allometric models to estimate the aboveground biomass of tropical trees *Glob. Change Biol.* **20** 3177–90
- Chave J, Muller-Landau H C, Baker T R, Easdale T A, Hans Steege T E R and Webb C O 2006 Regional and phylogenetic variation of wood density across 2456 neotropical tree species *Ecol. Appl.* **16** 2356–67

- de Assis R L, Wittmann F, Bredin Y K, Schöngart J, Nobre Quesada C A, Piedade M T F and Haugaasen T 2019 Above-ground woody biomass distribution in Amazonian floodplain forests: effects of hydroperiod and substrate properties *For. Ecol. Manage.* **432** 365–75
- De Souza F C *et al* 2016 Evolutionary heritage influences amazon tree ecology *Proc. R. Soc. B* **283** 20161587
- Díaz S *et al* 2016 New handbook for standardised measurement of plant functional traits worldwide *Aust. J. Bot.* **64** 715–6
- Dormann C F 2007 Effects of incorporating spatial autocorrelation into the analysis of species distribution data *Glob. Ecol. Biogeogr.* **16** 129–38
- Fan Z X, Zhang S B, Hao G Y, Ferry Slik J W and Cao K F 2012 Hydraulic conductivity traits predict growth rates and adult stature of 40 Asian tropical tree species better than wood density *J. Ecol.* **100** 732–41
- Ferraz A, Saatchi S S, Mallet C and Meyer V 2016 LiDAR detection of individual tree size in tropical forests *Remote Sens. Environ.* **183** 318–33
- Fick S E and Hijmans R J 2017 WorldClim 2: new 1 km spatial resolution climate surfaces for global land areas *Int. J. Climatol.* **37** 4302–15
- Friedlingstein P *et al* 2019 Global carbon budget 2019 *Earth Syst. Sci. Data* **11** 1783–838
- Gelman A and Rubin D B 1991 Inference from iterative simulation using multiple sequences *Stat. Sci.* **7** 457–511
- Gourlet-Fleury S *et al* 2011 Environmental filtering of dense-wooded species controls above-ground biomass stored in African moist forests *J. Ecol.* **99** 981–90
- Hacke U G, Sperry J S, Pockman W T, Davis S D and McCulloh K A 2001 Trends in wood density and structure are linked to prevention of xylem implosion by negative pressure *Oecologia* **126** 457–61
- Hawes J E, Peres C A, Riley L B and Hess L L 2012 Landscape-scale variation in structure and biomass of Amazonian seasonally flooded and unflooded forests *For. Ecol. Manage.* **281** 163–76
- Hietz P, Rosner S, Hietz-Seifert U and Wright S J 2017 Wood traits related to size and life history of trees in a Panamanian rainforest *New Phytol.* **213** 170–80
- Houghton R A, Byers B and Nassikas A A 2015 A role for tropical forests in stabilizing atmospheric CO<sub>2</sub> *Nat. Clim. Change* **5** 1022–3
- Jucker T *et al* 2018a Estimating aboveground carbon density and its uncertainty in Borneo's structurally complex tropical forests using airborne laser scanning *Biogeosciences* **15** 3811–30
- Jucker T, Bongalov B, Burslem D F R P, Nilus R, Dalponte M, Lewis S L, Phillips O L, Qie L and Coomes D A 2018b Topography shapes the structure, composition and function of tropical forest landscapes *Ecol. Lett.* **21** 989–1000
- Kellner J R *et al* 2019 New opportunities for forest remote sensing through ultra-high-density drone LiDAR *Surv. Geophys.* **40** 959–77
- Kellner K 2019 jagsUI: a wrapper around “rjags” to streamline “JAGS” analyses *R package version 1.5.1* (available at: <https://cran.r-project.org/package=jagsUI>)
- Lewis S L *et al* 2013 Above-ground biomass and structure of 260 African tropical forests *Phil. Trans. R. Soc. B* **368** 1625
- Magnabosco Marra D *et al* 2018 Windthrows control biomass patterns and functional composition of Amazon forests *Glob. Change Biol.* **24** 5867–81
- Martínez-Cabrera H I, Jochen Schenk H, Cevallos-Ferriz S R S and Jones C S 2011 Integration of vessel traits, wood density, and height in angiosperm shrubs and trees *Am. J. Bot.* **98** 915–22
- Mitchard E T A *et al* 2014 Markedly divergent estimates of Amazon forest carbon density from ground plots and satellites *Glob. Ecol. Biogeogr.* **23** 935–46
- Mitchard E T A, Saatchi S S, Baccini A, Asner G P, Goetz S J, Harris N L and Brown S 2013 Uncertainty in the spatial distribution of tropical forest biomass: a comparison of pan-tropical maps *Carbon Balance Manage.* **8** 1
- Mori G B, Schiatti J, Poorter L and Piedade M T F 2019 Trait divergence and habitat specialization in tropical floodplain forests trees *PLoS One* **14** e0212232
- Muñoz Mazón M, Klanderud K, Finegan B, Veintimilla D, Bermeo D, Murrieta E, Delgado D and Sheil D 2020 How forest structure varies with elevation in old growth and secondary forest in Costa Rica *For. Ecol. Manage.* **469** 118191
- Niklas K J and Spatz H C 2010 Worldwide correlations of mechanical properties and green wood density *Am. J. Bot.* **97** 1587–94
- Pan Y *et al* 2011 A large and persistent carbon sink in the world's forests *Science* **333** 988–92
- Patíño S *et al* 2009 Branch xylem density variations across the Amazon Basin *Biogeosciences* **6** 545–68
- Phillips O L, Sullivan M J P, Baker T R, Monteagudo Mendoza A, Vargas P N and Vásquez R 2019 Species matter: wood density influences tropical forest biomass at multiple scales *Surv. Geophys.* **40** 913–35
- Ploton P *et al* 2020 Spatial validation reveals poor predictive performance of large-scale ecological mapping models *Nat. Commun.* **11** 1–11
- Plummer M 2003 JAGS: a program for analysis of bayesian graphical models using Gibbs sampling *Proc. 3rd Int. Workshop on Distributed Statistical Computing* pp 20–22
- Raunonen P, Kaasalainen M, Markku Å, Kaasalainen S, Kaartinen H, Vastaranta M, Holopainen M, Disney M and Lewis P 2013 Fast automatic precision tree models from terrestrial laser scanner data *Remote Sens.* **5** 491–520
- Réjou-Méchain M *et al* 2019 Upscaling forest biomass from field to satellite measurements: sources of errors and ways to reduce them *Surv. Geophys.* **40** 881–911
- Saatchi S S *et al* 2011 Benchmark map of forest carbon stocks in tropical regions across three continents *Proc. Natl Acad. Sci.* **108** 9899–904
- Saatchi S S, Mascaró J, Xu L, Keller M, Yang Y, Duffy P, Espírito-Santo F, Baccini A, Chambers J and Schimel D 2014 Seeing the forest beyond the trees *Glob. Ecol. Biogeogr.* **24** 606–10
- Sæbo J S 2022 Data for: Ignoring variation in wood density drives substantial bias in biomass estimates across spatial scales *Mendeley Data* (<https://doi.org/10.17632/zzzzcnt2bd.1>)
- Slik J W F *et al* 2010 Environmental correlates of tree biomass, basal area, wood specific gravity and stem density gradients in Borneo's tropical forests *Glob. Ecol. Biogeogr.* **19** 50–60
- Sullivan M J P *et al* 2020 Long-term thermal sensitivity of Earth's tropical forests *Science* **368** 869–74
- Swenson N G and Enquist B J 2007 Ecological and evolutionary determinants of a key plant functional trait: wood density and its community-wide variation across latitude and elevation *Am. J. Bot.* **94** 451–9
- Tadono T, Ishida H, Oda F, Naito S, Minakawa K and Iwamoto H 2014 Precise global DEM generation by ALOS PRISM *ISPRS Ann. Photogram. Remote Sens. Spatial Inf. Sci.* **4** 71–76
- ter Steege H *et al* 2006 Continental-scale patterns of canopy tree composition and function across Amazonia *Nature* **443** 444–7
- Ubuy M H, Eid T and Bollandsås O M 2018 Variation in wood basic density within and between tree species and site conditions of exclosures in Tigray, northern Ethiopia *Trees* **32** 967–83
- Van Gelder H A, Poorter L and Sterck F J 2006 Wood mechanics, allometry, and life-history variation in a tropical rain forest tree community *New Phytol.* **171** 367–78
- van Nieuwstadt M G L and Sheil D 2005 Drought, fire and tree survival in a Borneo rain forest, East Kalimantan, Indonesia *J. Ecol.* **93** 191–201
- Walker W S *et al* 2020 The role of forest conversion, degradation, and disturbance in the carbon dynamics of Amazon indigenous territories and protected areas *Proc. Natl Acad. Sci.* **117** 201913321

- Watson C, Schalatek L and Patel S 2021 Climate finance thematic briefing: REDD+ finance *Clim. Finance Fundam.* **5** 1–4 (available at: <https://climatefundsupdate.org/>)
- Wiemann M C and Williamson G B 2002 Geographic variation in wood specific gravity: effects of latitude, temperature, and precipitation *Wood Fiber Sci.* **34** 96–107
- Wigneron J P, Fan L, Ciais P, Bastos A, Brandt M, Chave J, Saatchi S, Baccini A and Fensholt R 2020 Tropical forests did not recover from the strong 2015–2016 El Niño event *Sci. Adv.* **6** 112556
- Williamson G B and Wiemann M C 2010 Measuring wood specific gravity, correctly *Am. J. Bot.* **97** 519–24
- Wittmann F, Schöngart J, Parolin P, Worbes M, Piedade M T F and Junk W J 2006 Wood specific gravity of trees in Amazonian white-water forests in relation to flooding *IAWA J.* **27** 255–68
- Zanne A E, Lopez-Gonzalez G, Coomes D A, Ilic J, Jansen S, Lewis S L, Miller R B, Swenson N, Wiemann M C and Chave J 2009 Global wood density database *Dryad. Identifier* (available at: <Http://Datadryad.Org/Handle/10255/Dryad.235>)